An objective method for combining multi-parametric MRI datasets to characterize malignant tumors

Kathryn M. McMillan[a)]
Department of Radiology, Vanderbilt University, Nashville, Tennessee and Department of Medical Physics, University of Wisconsin, Madison, Wisconsin

Baxter P. Rogers
Institute of Imaging Science, Vanderbilt University, Nashville, Tennessee

Cheng Guan Koay
STBB/LIMB/NICHD, National Institutes of Heath, Bethesda, Maryland

Angela R. Laird
Research Imaging Center, University of Texas Health Science Center, San Antonio, Texas

Ronald R. Price
Department of Radiology, Vanderbilt University, Nashville, Tennessee

M. Elizabeth Meyerand
Department of Medical Physics, University of Wisconsin, Madison, Wisconsin

(Received 20 July 2006; revised 4 January 2007; accepted for publication 19 January 2007; published 23 February 2007)

Medical imaging has made significant contributions to the characterization of malignant tumors. In many cases, however, maps from multiple modalities may be required for more complete tumor mapping. In this manuscript we propose an objective method for combining multiple imaging datasets with the goal of characterizing malignant tumors. We refer to the proposed technique as the percent overlap method (POM). To demonstrate the power and flexibility of the POM analysis, we present four patients with recurrent glioblastoma multiforme. Each patient had multiple magnetic resonance imaging procedures resulting in seven different parameter maps. Chemical shift imaging was used to provide three metabolite ratio maps (Cho:NAA, Cho:Cre, Lac:Cre). A perfusion scan provided regional cerebral blood volume and permeability maps. Diffusion and carbogen-based hypoxia mapping data were also acquired. Composite maps were formed for each patient using POM, then were compared to results from the ISODATA clustering technique. The POM maps of likely recurrent tumor regions were found to be consistent with the ISODATA clustering method. This manuscript presents an objective method for combining parameters from multiple physiologic imaging techniques into a single composite map. The accuracy of the map depends strongly on the sensitivity of the chosen imaging parameters to the disease process at the time of image acquisition. Further validation of this method may be achieved by correlation with histological data. [DOI: 10.1118/1.2558301]

I. INTRODUCTION

Frequently, a single imaging modality is not adequate to uniquely differentiate normal from cancerous tissue. Numerous studies have shown that the combined information from multiple images can yield improved discrimination of diseased tissue.[1–4] However, when multi-parametric studies are utilized, the amount of data can be overwhelming and potentially lead to inappropriate and inconsistent interpretation. We present a method based on overlapping regions of thresholded parameter maps that is a fast, easily implemented technique for combining the most useful results from multi-parametric datasets into a single map. We refer to this technique as the percent overlap method (POM).

Previous studies have shown improved sensitivity from combining techniques compared to a single image.[1–4] The approach of these multi-parametric studies generally was to use region of interest based analyses to find correlations between physiologic parameters rather than to provide the single composite map proposed here.

Recurrent tumors undergo time-dependent evolution.[5] Parameter efficacy is therefore likely to change over time as tumors grow, mature, necrose or continue to infiltrate into surrounding brain tissue. Glioblastoma multiformes (GBMs) in particular are quite heterogeneous; certain areas show aggressive behavior, while other regions show little evidence of progression. The *a priori* selection of the optimal parameter at a given time point is difficult, therefore results of multi-parametric studies are more likely to discriminate diseased from normal tissue.

The underlying assumption of POM is that the specificity to voxels representing recurrent disease will be increased by the use of multiple techniques. There is therefore the task of reducing the amount of information gained from multiple scans while retaining the most tumor-specific information. In the POM technique, this reduction of the dataset to a composite map is performed through combining binary maps made of thresholded physiologic parameters.

In this manuscript, we have chosen to compare the POM with a more conventional method of incorporating multiparametric datasets into a composite map, ISODATA. While alternate segmentation algorithms are available, including various applications of automated methods,[6,7] ISODATA was chosen over other clustering approaches since it does not require knowledge of the number of clusters *a priori*.[8] ISODATA is an iteratively self-organizing variation of the K-means algorithm, and has previously been validated in stroke patients.[9–11] Since highly descriptive parameters vary from patient to patient in both identity and quantity, an self-adjusting algorithm is particularly important.

Both POM and ISODATA are capable of providing maps descriptive of the extent and environment in recurrent tumors. We believe the specific physiologic parameters chosen in this study to be predictive of tumor metabolism, proliferative potential, cellularity, and oxygenation status, which we obtained via chemical shift imaging (CSI), perfusion, diffusion and hypoxia scans. Our hypothesis is that the same locations would be identified as recurrent disease by both POM and ISODATA methods. In addition, through the comparison of the two techniques in the same patients, strengths and weaknesses of each method can be illustrated.

II. METHODS

To demonstrate the composite mapping techniques, we have chosen patients with recurrent high-grade primary brain tumors, specifically GBM. We have chosen to investigate the following parameters: CSI, diffusion-weighted images, perfusion-weighted images and blood oxygenation level dependent (BOLD)-based hypoxia maps. Each parameter has previously been used by other investigators for characterizing brain tumors.[1–4,12–15,17]

The study is an IRB approved clinical protocol, and all subjects provided informed consent. Magnetic resonance (MR) scanning was performed on a clinical 1.5T GE Signa Horizon magnet (GE Medical Systems, Milwaukee, Wisconsin) equipped with gradients for whole-body echo-planar imaging (EPI). The multi-parametric dataset was composed of chemical shift imaging ratio maps (Choline:Creatine, Choline:NAA, Lactate:Creatine), apparent diffusion coefficient (ADC) maps from diffusion-weighted imaging, permeability and regional cerebral blood volume (rCBV) maps from a dynamic contrast enhanced perfusion techniques, and a BOLD based method provided the hypoxia maps.

Patient 1 was a male, age 53, being followed after surgery for the initial disease. Postsurgical histology confirmed the GBM diagnosis. External beam radiation therapy was completed, and the multi-parametric dataset was acquired 12 months postradiotherapy. This scan revealed progression of the tumor and further surgery confirmed GBM recurrence around the rim of the resection cavity.

Patient 2 was a 47-year-old male diagnosed with GBM after previously being treated for a low-grade glioma. The scan acquired 7 months postsurgery showed an enhancing lesion posterior to the more frontal resection bed. The second progression was confirmed to be GBM at subsequent surgery.

Patient 3 was a female, age 63, who was initially treated for GBM with surgery and external beam radiation therapy, then recurred. Our study began 4 months after stereotactic radiosurgery for this recurrence. Conventional follow-up scans revealed a likely recurrent region 7 months postradiosurgery and a craniotomy confirmed the presence of disease.

Patient 4 was a 43 year old female. She was treated with a craniotomy and subsequent radiation therapy. Enrollment in the POM study occurred two years postsurgery. Conventional followup scans failed to indicate recurrence at any of the follow-up time points acquired over three years. We therefore show a POM from a time point 58 months postsurgery.

A. CSI protocol

The scan parameters for the PRESS CSI acquisition were TR=1.0 s, echo times (TE)=144 ms, ϕ=90°, volume matrix=18×18. Voxels dimensions were 1.5×1.5×1.5 cm^3. The PRESS volume was prescribed based upon contrast-enhancing regions on T1-weighted images. The volume of tissue studied varied over patients and tumor locations, and full brain coverage never achieved. Postprocessing consisted of compensation for residual eddy currents, Gaussian line broadening (time constant, 256 ms), and zero- and first-order phase correction after two-dimensional Fourier transformation.[12] For each voxel, spectroscopic analysis was used to establish the relative areas of peaks corresponding to NAA, choline, creatine, and lactate. Metabolic images were formed from the real parts of the spectra after phase and base line corrections (least squares method) by integration of the signal within the spectral area of the particular metabolite. Three ratio maps (Choline:NAA, Choline:Creatine and Lactate:Creatine) were formed for the POM.

B. Diffusion protocol

Diffusion-weighted EPI images were acquired with the parameters as follows: TR=5 s, TE=86 ms, ϕ=90°, field of view (FOV)=22 cm, slice=5 mm, gap=0 mm, matrix=256×256, b=0 and 1000 s/mm^2. Diffusion gradients were applied in the three orthogonal directions. These acquisition parameters of the multi-slice technique resulted in whole brain coverage. Diffusion-weighted images were reduced to ADC maps for comparison across patients.[13]

C. Perfusion protocol

Perfusion-weighted images were acquired over the whole brain in the axial plane using the acquisition parameters TR=2 s, TE=60 ms, ϕ=60°, FOV=22 cm, slice=7 mm, gap=2 mm, matrix=128×128. Contrast of 0.1 mmol/kg of body weight of a gadodiamide (Omniscan, Nycomed-Amersham, Princeton, NJ) was injected at 4.0 ml/s followed by a saline flush using a power injector (Spectris, MEDRAD, Indianola, PA) 13 s after scan initiation.

We created maps of regional cerebral blood volume (rCBV) using a bolus method. The arterial input function (AIF) was automatically detected based on a standard deviation threshold of signal change.[14] The area under the AIF is used to normalize the tissue curve such that:

$$\mathrm{rCBV} = k/\alpha^{*} \int (C_{\mathrm{tissue}}(t)dt) / \int (C_{\mathrm{AIF}}(t)dt),$$

where k/α are physiological constants that depend on the blood hematocrit and brain tissue density, C_{tissue} is the gadolinium concentration in tissue and C_{AIF} is the gadolinium concentration in the AIF.

Li's[15] first pass leakage profile method was used to calculate permeability maps using

$$C_t(t) = K_{\mathrm{trans}} \int C_p(t')dt' + v_p C_p(t),$$

where C_t is the time course curve of the contrast agent concentration, K_{trans} is the volume transfer constant between the plasma and extracellular extravascular space as calculated from the first pass model, C_p is the tracer concentration in arterial blood plasma, v_p is the volume of blood plasma per tissue unit volume.[15]

D. Hypoxia mapping protocol

Hypoxia maps were obtained via a multi-echo EPI sequence with ten different echo times (TE) to quantify $T2^{*}$. Parameters were as follows: TR=2 s, TE=35–80 ms (steps of 5 ms), ϕ=90°, FOV=22 cm, slice=5 mm, gap=1 mm, matrix=128×128 for full brain coverage. The patient breathed carbogen (95% O_2, 5% CO_2) through a tube placed in the mouth in order to modulate oxygenation in hypoxic areas.

Differences between air and carbogen scans are specific to hypoxic areas since oxygenation levels will remain unchanged in normal tissue as well as necrotic areas.[16] During the air-breathing interval, the tube was not attached to the patient, allowing room air breathing. The tube then connected the patient to the carbogen tank and the gas flow was adjusted to a rate of 20 l/min for the equilibration and carbogen breathing intervals. The patient was instructed to breathe only through his mouth at those times. Nose clips were used in later patient scans to ensure compliance. EPI images were initially acquired with normal air breathing. The patient then breathed carbogen gas for a 15 min equilibration period before the next EPI scan began. The patient continued to breathe the carbogen gas during the acquisition of the second set of multi-echo EPI images.

$T2^{*}$ was calculated for air and carbogen breathing by fitting the signal intensity (SI) vs echo time (TE) to a single exponential function using MATLAB (Mathworks Corp., Natick, MA) according to the equation

$$\ln[\mathrm{SI}(1)] = -\mathrm{TE}/\mathrm{T2} + \ln[\mathrm{SI}(0)],$$

where SI(0) and SI(1) are the signal intensities at time 0 and 1, respectively.[17] Relative changes between air and carbogen breathing were evaluated using a paired Student's t test.

E. Percent overlap method (POM)

We hypothesized that if a voxel contained a recurrent tumor, multiple parameter maps would contain an extreme parameter (i.e., maximum or minimum) value as determined by thresholding based on the undiseased hemisphere. To account for different acquisition resolutions, each dataset was resampled (1 mm^3 voxels) and aligned to a high-resolution anatomical scan (postcontrast, T1-weighted SPGR acquired with the following parameters: TR=21 ms, TE=6 ms, flip angle=20°, FOV=24 cm, slice thickness=1.5 mm, gap =0 mm, matrix=256×256).

To minimize registration error due to motion within a single scan session, the head was immobilized with straps and foam padding before the first scan was acquired. Images were registered by aligning common neuroanatomic landmarks. Acquiring images from the whole-brain volume for perfusion, diffusion, and hypoxia data gave an increased number of landmarks. Due to shimming constraints, spectroscopy data were acquired in a smaller region placed around the abnormally enhancing area. AFNI was used to manually align physiologic data to the high-resolution T1-weighted image when viewed in three planes.[18] A rigid body transformation used 6 degrees of freedom, 3 for linear shifts and 3 for angular rotations. The CSI data were acquired in a smaller region of interest and the prescribed parameters of extent were used to overlay the metabolite maps on the anatomical images.

After registration, the POM method was completely automated and required no user interaction as whole brain maps were created. Using a standard desktop computer running MATLAB, maps were available after approximately 5 min. The entire contralateral (nontumor) hemisphere was used to establish appropriate thresholds for each parameter by selecting the same percentile value (i.e., 95th percentile for the maps shown) for each resampled and aligned parameter map. Since each resampled parameter map except CSI contained the same number of voxels, the same quantity of tissue was selected for each whole brain technique by selecting threshold levels based on percentiles. Binary maps were then formed by thresholding each parameter map to contain only the extreme values (high Choline:NAA, Choline:Creatine, Lactate:Creatine, high rCBV, high permeability, low ADC, and highly significant $T2^{*}$ differences for hypoxia) such that surprathreshold voxels were equal to one, and all others were zero. Each thresholded parameter map contains a certain number of voxels, called Voxels_x, where x is the individual parameter (e.g., ADC, rCBV, hypoxia).

A single composite map containing all seven parameters was formed where the signal intensity indicated the parameters that overlapped in each voxel. Unique values were first assigned to each of the seven thresholded parameter maps (e.g., permeability=1, hypoxia=2, Cho:Cre=4, Cho:NAA=8, Lac:Cre=16, rCBV=32, ADC=64) and sums were calculated. A unique value then existed for every possible combination of techniques. The assignment of unique values allowed for the determination of which parameters

TABLE I. Shows the percent overlap for Patient 3 in both healthy and tumor hemispheres. The selection of parameters for inclusion into the final map was based upon those maps which exhibited higher overlap in the tumor compared to the healthy hemisphere. After ensuring the tumor hemisphere exceeded the healthy hemisphere in overlap percentages, the four techniques with the highest overlap were included in the final map for this patient.

Parameter	Value	Healthy	Tumor
Permeability	1	4%	19%
Hypoxia	2	45%	91%
Cho:Cre	4	73%	93%
Cho:NAA	8	87%	100%
Lac:Cre	16	42%	40%
rCBV	32	34%	34%
ADC	64	17%	18%

overlapped from color coding based upon which pure parameter maps contributed to the sum in each voxel. Voxels for each value were then counted.

The percent overlap was calculated for each technique x, using

$$\text{Percent Overlap} = (\text{Voxels}_x - \text{Voxels}_{\text{only}x})/\text{Voxels}_x,$$

where Voxels_x was defined previously as the total number of voxels in a thresholded parameter map, and $\text{Voxels}_{\text{only}x}$ counts the voxels for technique x that do not show overlap with any other technique. Therefore, the numerator gives the number of voxels that overlap with any other technique and the denominator counts every voxel in the thresholded map regardless of overlap.

F. Assessing parameter map utility

Calculations of overlap percentage were performed for each hemisphere separately for each parameter. A parameter was considered successful in mapping physiology of interest if the disease hemisphere showed increased overlap compared to the contralateral hemisphere. When considering the 28 physiologic maps from the four patients presented, a single map had higher percent overlap in the normal hemisphere. There were equal overlap percentages between hemispheres for three maps. Table I lists the overlap values obtained for Patient 3 and illustrates how four parameter maps were selected for inclusion in a final POM map.

While an unlimited number of input techniques are feasible when implementing POM, the color coding for the final map becomes confusing when including more than four input parameters and the possible combinations thereof. After examination of overlap values and selection of techniques likely to be specific to tumor areas containing the highest percent overlap, POM maps were formed in AFNI.[18] The top four overlap values were chosen unless fewer techniques yielded an overlap percentage less than or equal to the contralateral value. Voxels containing overlap are displayed as functional overlays with corresponding color bars.

Figure 1 illustrates the POM in two steps for Patient 3. A high-resolution postcontrast T1-weighted image is used for reference and shows several areas of enhancement around the original tumor site. Whole brain parameter maps (L-R: permeability, hypoxia, Cho:Cre, Cho:NAA) are thresholded at the 95th percentile of intensity values in the healthy hemisphere. Each map was reduced to the extreme values (i.e., only voxels with values exceeding 95% of the maximum of the value derived from the undiseased hemisphere are retained) and assigned a unique number (L-R: high permeability=1, high $\Delta T2^*$=2, high Cho:Cre=4, high Cho:NAA=8). These binary maps were added to create a composite map where the voxel value represents the number and identity of overlapping techniques. Voxels with a value of 13 indicate an overlap of Cho:NAA, permeability and Cho:Cre (displayed in the POM map as orange), while yellow voxels would have a value of 5, from an overlap of Cho:Cre and permeability.

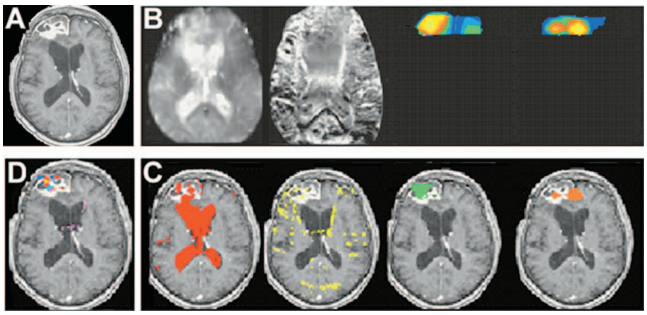

FIG. 1. Percent overlap method. (A) A high-resolution postcontrast T1-weighted image is used for reference and all parameter maps are resampled and aligned to match this scan. (B) Whole brain parameter maps (L-R: permeability, hypoxia, Cho:Cre, Cho:NAA) are thresholded to contain the maximum 5% of voxels to obtain (C). Voxels with values of parameter maps exceeding 95% of the undiseased hemisphere extreme value presented as a color-coded overlay on the postcontrast T1 image. Each thresholded parameter map is assigned a unique number (e.g., 1=permeability, 2=hypoxia, 4=Cho:Cre, 8= Cho:NAA), then unions are calculated to create (D) a composite map where voxels displayed contain more than one thresholded parameter map, color coded to indicate the identity of the maps in (C) that overlap.

G. ISODATA clustering analysis

We have chosen to compare the POM results with ISODATA, an iteratively self-organizing variation of the *K*-means algorithm, since this clustering technique has been validated against histology when considering multiparametric datasets in stroke patients.[9–11] ISODATA places each parameter on a separate axis, creating an n-dimensional space describing the tissue. Different tissue types can be differentiated by the parameter clusters in the n-dimensional parameter space. Details on the method are available in Jacobs *et al.*[10] and Mitsias *et al.*[11] As described in Shen *et al.*, the lumping parameter was chosen by defining a region of interest in the dominant tissue type for a given slice. The standard deviation parameter was then selected based upon another tissue type within that slice.[19]

Eigentool image processing software (Henry Ford Hospital, http://www.radiologyresearch.org/eigentoolhelp/) was used to perform the ISODATA analysis. The multiparametric images were considered slice by slice, and in-

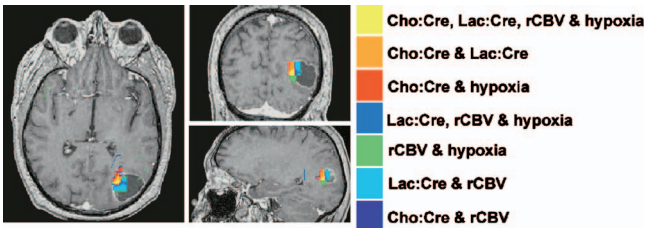

FIG. 2. Patient 1 POM composite map. Abnormal voxels from Cho:Cre, Lac:Cre, rCBV and hypoxia parameter maps for Patient 1. POM map overlaid on postcontrast T1. Yellow voxels, abnormal in all four parameter maps, are most compelling, but insight into the heterogeneous environment is offered by other colors showing overlap among various parameter maps. There appear to be regions of microscopic extension extending medial to the enhancing rim of the surgical bed.

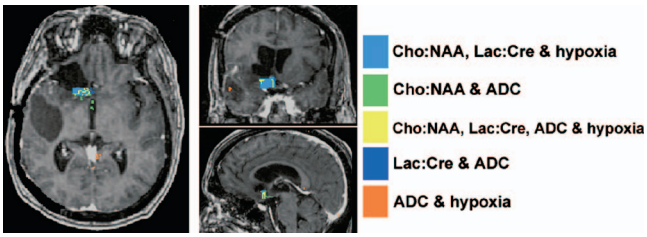

FIG. 3. Patient 2 POM composite map. POM map for Patient 2 shows a region of interest posterior to the most frontal of the resection cavities. The regions containing yellow voxels, abnormal in all four parameter maps, are most compelling. A large cluster is defined by the spectroscopy ratio maps and the hypoxia scan, and could direct specific attention to that corner of the resection cavity when planning treatment.

cluded anatomical as well as physiologic maps such that the dataset for each patient included a postcontrast T1-SPGR, postcontrast T2-FLAIR, ADC, rCBV, permeability, hypoxia, Cho:NAA, Cho:Cre, and Lac:Cre. A second clustering analysis was completed using only the four parameters containing the highest percent overlap from the POM. Using a Sun workstation, the user is required to enter initial parameters, then the analysis takes less than 1 min per slice. However, when our goal was to obtain whole brain maps, up to 80 slices resampled to match the high-resolution anatomical grid could require organization and processing, creating a considerably labor-intensive process.

Two theme maps per patient resulted from these analyses, where different clusters are shown by different colors.[10] While the number of input parameters was constant over patients, the identity of the four physiologic maps included in the ISODATA analysis was determined by the percent overlap calculations.

The Kappa Statistic[20] was used to determine if the POM maps defined areas similar in location to those identified by the clustering algorithm. The assumption is that if our thresholding values were appropriate and the relevant techniques were chosen, similarly appearing maps would result from both POM and ISODATA clustering. Area measurements were obtained slice by slice for overlap composite maps and for clusters on ISODATA theme maps. When viewing the techniques on the same underlying image, inclusive and exclusive voxels were counted and used to calculate kappa.

III. RESULTS

Figure 2 displays a three-axis view of the POM composite map for Patient 1 from a scan acquired six months post-therapy. The color-coded map utilized the extreme 5% of values from each selected parameter map. The rim of the resection bed shows enhancement on the T1-weighted image. Voxels along the interior edge show overlapping combinations: Lac:Cre overlaps with rCBV in cyan; Lac:Cre, rCBV and hypoxia overlap in blue; Cho:Cre with rCBV (indigo), and Cho:Cre with hypoxia (red). RCBV/hypoxia overlap is found near the inferior portion of the overlapping region in green, while a medial band of orange shows Cho:Cre and Lac:Cre voxels. The central yellow region shows overlap of all four parameters.

Figure 3 displays a three-axis view of the overlap composite map for Patient 2 acquired seven months postresection, using a 5% threshold. Four parameters met the selection criteria including Cho:NAA and Lac:Cre—both with 97% overlap, hypoxia at 27% and 23% overlap in ADC. Voxels showing these overlaps are seen in an enhancing region posterior to the most frontal resection cavity. Regions of overlap between the Lac:Cre, Cho:NAA and hypoxia are found in all slices colored cyan. Yellow voxels represent Cho:NAA, Lac:Cre, ADC and hypoxia overlap and are found toward the interior edge of the overlap region in Fig. 3. Dark blue regions show Lac:Cre and ADC overlap. More subtle overlaps include voxels in orange (ADC and hypoxia) as well as regions displaying Cho:NAA and ADC shown in green.

Permeability, hypoxia, Cho:NAA and Cho:Cre were selected from the seven parameter maps for Patient 3 at the recurrent time point acquired seven months post-stereotactic radiosurgery for Fig. 4. Areas of overlap are seen in the enhancing areas. Hypoxia and permeability overlap in ventricle areas, likely reflecting blood flow effects from each technique. When considering hypoxia and permeability maps alone, however, many additional areas would need to be ex-

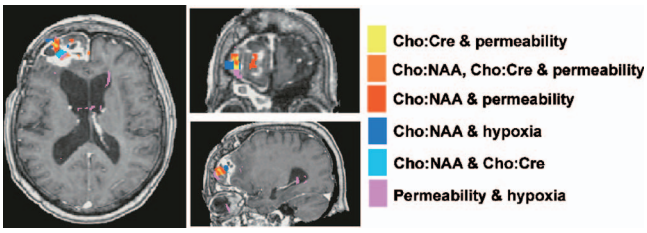

FIG. 4. Patient 3 POM composite map. Physiology of interest within the central portion of the enhancing region for Patient 3. Permeability is thought to be a biomarker for immature, leaky vasculature. Correlations with areas of high cell turnover as measured by Choline, and areas of hypoxia are seen. Using a 5% threshold, Cho:NAA showed 100% overlap, Cho:Cre – 93%, permeability – 19%, hypoxia – 91%. Voxels in and around the ventricles show overlap between permeability and hypoxia (violet) thought to relate to blood flow effects.

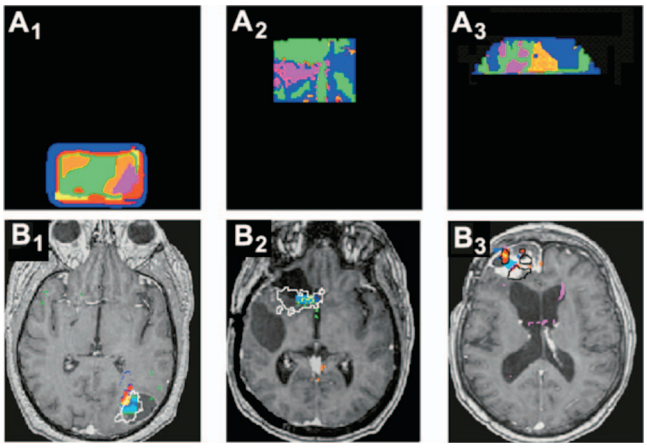

FIG. 5. ISODATA vs POM. ISODATA results are shown in the top row for patients 1 (A_1), 2 (A_2) and 3 (A_3). An outline of the ISODATA result was placed on the corresponding POM map for comparison, B_{1-3}. There is some mismatch in spatial location, but the same general areas are found.

amined for lack of specificity. The overlap map decreases the chances of returning areas not corresponding to tumor processes.

The comparison of POM to ISODATA maps for each of three patients is presented in Fig. 5. The Kappa statistic[20] indicates significant agreement between ISODATA results and POM maps, specifically Kappa=0.932, 0.854, and 0.842 for patients 1, 2 and 3, respectively.

Figure 6 shows Patient 4 three years postradiotherapy with no indications of progression (A). The stability of that time point was also suggested by a scan acquired four months later (B). Individual thresholded maps found no large areas of concern (C-F), nor does the overlap image. Therefore, even when using a moderate 5% threshold for the maps, areas which should not appear in the maps are largely absent. Overlap therefore seems to be contained to areas of likely recurrence in our patient population.

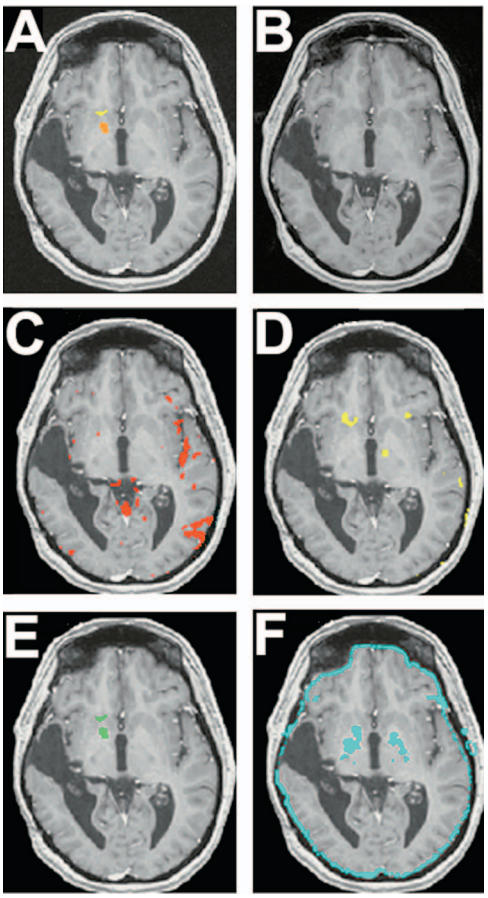

FIG. 6. No recurrent tumor POM composite map. A representative POM map at a stable time point is shown for Patient 4(A). Orange voxels indicate overlap between the Cho:NAA and ADC maps. Yellow voxels represent Cho:NAA and hypoxia overlap. The corresponding slice from a future scan acquired at a four month interval (B) is also shown to indicate this patient's stability over time after the nonspecific overlap map. Parameters of possible interest appeared to be rCBV (C), hypoxia (D), Cho:NAA (E) and ADC (F). Overlap percentages tend to be lower than those seen in recurrent patients and composite maps show no areas of particular interest. Also note that while the rCBV map does not overlap with the other physiologic maps, its inclusion does not affect other POM voxels.

IV. DISCUSSION

An accurate, rapid and objective method for condensing information from multi-parametric studies for use in diagnosis or treatment planning is critical for large-scale implementation. We present results from the percent overlap method (POM) as a potential candidate.

When many parameters are considered for recurrent brain tumor patients, the amount of information can become overwhelming and therefore of limited use. Combining multiple parameters in an easy to read map is therefore desirable for use in radiology, neurosurgery, oncology, and radiation treatment planning. By finding the most appropriate techniques at every time point, the number of parameters of interest can be reduced in an easily standardized way.

The threshold percentile chosen to select extreme values from the individual parameter maps may introduce a degree of subjectivity. A concern with this approach is that the POM could neglect some recurrent areas since the complementary nature of the individual parameters is neglected in order to focus on redundant information. However, falsely positive areas could be largely avoided due to the nature of the overlap calculations because of the same reliance on parameter redundancy.

In future studies, POM subjectivity could be minimized by accurate histologic confirmation. Though GBM recurrence was confirmed by subsequent surgery for each of the patients studied here, detailed histologic information describing true extent and environment was not available. Due in part to the lack of detailed histological verification in our patient population, we have also chosen to present a comparison to the POM via the ISODATA technique.

Since a majority of GBM patients recur locally, we expected to see voxels highlighted in composite maps located close to the resection bed.[21] Three patients displayed this

pattern, and recurrence was confirmed by subsequent surgery. Since diffusion, perfusion and hypoxia scans were acquired for the whole brain, there was the potential to detect distal recurrences as well. Spectroscopy appears to offer an advantage in its specificity to the recurrent locations, but was only acquired in a region prescribed around the contrast-enhancing abnormality. Advances in CSI acquisition should make composite mapping strategies stronger.

The overlap map from Patient 1 suggests certain regions could be outgrowing their blood supplies and forming hypoxic conditions where anaerobic metabolism is necessary. High Choline was found near these regions, overlapping with hypoxia, rCBV, both hypoxia and rCBV, and both Lac:Cre and rCBV. An overlapping area of hypoxia and high blood volume was located near the hypoxia and Lac:Cre region, possibly relating to leaky neovasculature promoted by hypoxic conditions.[16]

Further treatment was initiated for Patient 1 when recurrence was diagnosed using the conventional images acquired during the first follow-up scan after completing radiation therapy. Physiologic parameters supported the diagnosis, and regions of interest are seen in the composite map. Lactate levels are elevated in many hypoxic regions lending support to the hypothesis of an oxygen-starved environment in these areas. Tumor blood vessels are highly irregular, have arteriovenous shunts and blind ends, and lack normal smooth muscle;[22] as a result, tumor blood flow is highly variable. Since BOLD-based hypoxia mapping has not been used extensively in humans, overlap with relevant techniques provides some support for its utility by relating it to previously validated parameter maps.

BOLD-based hypoxia maps are not currently used clinically to our knowledge. Ongoing research indicates that changes in response to hyperoxygenation in well oxygenated and necrotic regions would be expected to be relatively small in comparison to the hypoxic tumor regions. If vessels are highly constricted or blocked, or if regions are lacking vasculature or contain highly immature vessels, they experience no vasodilation. Therefore, there is no signal change. Additional areas which do not respond to carbogen are necrotic areas with paramagnetic breakdown products. These appear as bright regions on $T2^*$ maps. Dark regions are cystic or have low cellular density.[23] Well perfused, oxygenated regions also show no significant signal changes since improvements in oxygenation cannot occur to a great degree.[24]

The map for Patient 2 shows voxels containing a combination of Cho:NAA, Lac:Cre, decreased ADC and hypoxia, suggesting the presence of areas with high cell turnover that could resort to anaerobic metabolism when competition for nutrients and oxygen becomes too severe. More medial regions of Cho:NAA and hypoxia overlap voxels could further indicate increased cell turnover resulting in lack of oxygen to some cells. Areas showing high Lac:Cre, hypoxia and low ADC could possibly indicate dense cellularity, creating an environment lacking in oxygen and nutrients, therefore promoting anaerobic metabolism. While ADC has been unreliable in differentiating infiltration from surrounding edema,[25] it still has potential value in composite maps such as these. While many parameters may be introduced that show a lack of specificity or reliability, considering them as part of a set of parameters allows overlap measures to increase the knowledge of underlying physiology. This could aid in the evaluation of parameter utility on a patient-by-patient basis.

Patient 3 shows several regions of interest. There are very small areas of overlap between high permeability and Choline ratio maps. The larger region shows hypoxic abnormalities. These areas appear highly localized to the enhancing region with the exception of the purple voxels likely showing blood flow effects in hypoxia and permeability maps. Permeability is thought to be a measure of angiogenesis induced by hypoxic environments. Since hypoxia could result from densely cellular areas, the overlap among these four parameters is reasonable.

Whole-brain maps may be obtained very quickly with the POM. In addition, analysis of the individual maps could be aided through comparison to the composite map regions. Though the ISODATA technique has been extended to order clusters in terms of the probability that they contain normal tissue,[11] the POM maps offer descriptive information in terms of which parameters indicate recurrence at specific voxels.

The POM introduces subjectivity in selecting extreme values of each technique. However, when considering that extreme values are important in many of the parameters, reducing the maps to only the maximum values (or minimum values in ADC maps) appears to be a valid method at combining parameters. In addition, this thresholding step allows some control over the area defined as abnormal on the final composite maps. Lowering the threshold, and therefore increasing the number of voxels that are allowed to participate in overlap composite maps, will increase the areas obtained from the overlap technique.

The 5% threshold was initially utilized since it appeared to find relevant voxels but did not cause an appreciable amount of noise in the contralateral hemisphere. Without independent hypothesis testing and verification, we found the 5% threshold was a viable compromise. If histologic confirmation of tumor extent was available, the composite map area could be optimized to highlight the truly important areas.

POM is insensitive to the addition of parameters that do not indicate recurrent disease. However, adding irrelevant parameters to ISODATA limited its ability to find the abnormal clusters. When using all seven physiologic parameter maps and the two anatomical scans in the ISODATA algorithm, a single cluster appeared for the entire region. In our small group of patients, ISODATA appears to be of limited use when irrelevant parameter maps are added. Conversely, overlap maps were insensitive to the inclusion of irrelevant parameters. We have limited our input to four maps for ease of reading the corresponding color bar, but additional parameters could be added and more colors assigned to the various

overlapping regions. If techniques are not found to be useful, they would be unlikely to overlap with the other component techniques, but the other concordant voxels would remain unaffected.

Patient 4 suggests the specificity of the POM to likely recurrent areas. Thresholding nonspecific physiologic parameter maps and their subsequent combination into a single composite map failed to show any large areas of interest. For each of our patients, the typical follow-up scans acquired at three-month intervals failed to produce POM maps of interest until the final imaging time point where treatment was initiated due to the suggestion of recurrence based upon standard imaging methods.

Clustering methods have previously been shown to be useful for combining multiple parameters, and have demonstrated their utility in stroke studies in human and animals.[8–11] However, current programs accept information slice by slice, adding some organization issues and losing efficiency when multi-slice maps are needed. Since tumor physiology is heterogeneous, a whole brain strategy using small voxel volumes may be optimal. If whole-brain processing can occur with overlap methods, and comparable maps result from an ISODATA algorithm, the ease and speed of considering overlapping voxels makes the POM a feasible choice.

An efficient way of using ISODATA to select for the most tumor-specific parameters is not immediately apparent. While the maps could be considered independently and clustering results examined for each technique, considering multiple slices would involve considerable time. If diffusion measurements are corrupted by peritumoral edema, or if rCBV results are not specific to tumor areas, it would be difficult to determine their efficacy at particular time points.

ISODATA also suffers from some degree of subjectivity in the selection of input parameters. The technique failed in several slices for each patient when standard deviation and lumping parameters were not ideally selected. Additionally, there must be some subjectivity introduced to interpret the ISODATA clusters. While the overlap offers a color bar to determine which techniques contributed to the selection of voxels as abnormal, it is difficult to determine which parameters determined the cluster size and location in ISODATA theme maps.

In addition, areas of extreme values for single component parameters could be viewed for the overlap maps to determine if the complementary nature of the techniques indicates a greater spatial extent for recurrence. While many of these parameters seem to be somewhat redundant, one of the major reasons for using multi-parametric datasets is to find information not offered by other techniques. If a particular map strongly indicates recurrence, it could be viewed in its entirety along with the overlapping voxels from other techniques. Overlap maps would then serve to cue nonradiologically trained personnel to check certain regions on the individual component maps more carefully if they are near areas highlighted on the POM composite map.

V. CONCLUSION

We have shown that the POM offers a fast, easily implemented method for combining multiple parameters into a single map that reflects the probability of abnormality. The confirmation that ISODATA clustering techniques isolate similar regions gives confidence that overlap methods are robust. The question of true spatial extent is a critical one, especially since the there can be optimization of the cluster area returned from the POM. Histologic measurements will be necessary to map true extent for comparison with multiparametric techniques for combination, but we offer a simple technique that enables clinical staff to utilize physiologic imaging parameters.

ACKNOWLEDGMENTS

The authors are grateful for grant support from NIH/NINDS 5F31 NS046168-02, NIH/NCI 2R25 CA092043-06.

[a]Author to whom correspondence should be addressed. Electronic mail: kathryn.mcmillan@vanderbilt.edu

[1]R. Gupta, U. Sinha, T. F. Cloughesy, and J. R. Alger, "Inverse correlation between choline magnetic resonance spectroscopy signal intensity and the apparent diffusion coefficient in human glioma," Magn. Reson. Med. **41**, 2–7 (1999).

[2]D. Yang *et al.*, "Cerebral gliomas: Prospective comparison of multivoxel 2D chemical-shift imaging proton MR spectroscopy, echoplanar perfusion and diffusion-weighted MRI," Neuroradiology **44**, 656–666 (2002).

[3]M. Castillo, J. K. Smith, L. Kwock, and K. Wilber, "Apparent diffusion coefficients in the evaluation of high-grade cerebral gliomas," AJNR 2001; 22, 60–64 (2001).

[4]R. G. Henry *et al.*, "Comparison of relative cerebral blood volume and proton spectroscopy in patients with treated gliomas," AJNR 21, 357–366 (2000).

[5]L. E. Gaspar *et al.*, "Supratentorial malignant glioma: Patterns of recurrence and implications for external beam local treatment," IJROBP 24(1), 55–57 (1992).

[6]J. Liu, J. K. Udupa, D. Odhner, D. Hackney, and G. Moonis, "A system for brain tumor volume estimation via MR imaging and fuzzy connectedness," Comput. Med. Imaging Graph. **29**, 21–34 (2005).

[7]A. Stadlbauer, E. Moser, S. Gruber, R. Buslei, C. Nimsky, R. Fahlbusch, and O. Ganslandt, "Improved delineation of brain tumors: An automated method for segmentation based on pathologic changes of H1-MRSI metabolites in gliomas," Neuroimage **23**, 454–461 (2004).

[8]H. Soltanian-Zadeh *et al.*, "MRI tissue characterization of experimental cerebral ischemia in rat," J. Magn. Reson Imaging **17**, 398–409 (2003).

[9]Q. Shen, H. Ren, M. Fisher, J. Bouley, and T. Duong, "Dynamic tracking of acute ischemic tissue fates using improved unsupervised ISODATA analysis of high-resolution quantitative perfusion and diffusion data," J. Cereb. Blood Flow Metab. **23**, 887–897 (2004).

[10]M. A. Jacobs *et al.*, "A model for multiparametric MRI tissue characterization in experimental cerebral ischemia with histologic validation in rat," Stroke **32**(4), 943–957 (2001).

[11]P. D. Mitsias *et al.*, "Multiparametric MRI ISODATA ischemic lesion analysis," Stroke **33**(15) 2839–2844 (2002).

[12]M. T. Shih, A. K. Singh, A. M. Wang, and S. Patel, "Brain lesions with elevated lactic acid peaks on magnetic resonance spectroscopy," Curr. Probl Diagn. Radiol. **33**, 85–95 (2004).

[13]T. Sugahara, T. Korogi, and M. Kochi, "Usefullness of diffusion-weighted MRI with echo-planar techniques in the evaluation of cellularity in gliomas," J. Magn. Reson Imaging **9**, 53–60 (1999).

[14]T. J. Carroll, H. A. Rowley, and V. M. Haughton, "Automatic calculation of the arterial input function for cerebral perfusion imaging with MRI," Radiology **227**, 593–600 (2003).

[15]K. L. Li, X. P. Zhu, J. Waterton, and A. Jackson, "Improved 3D quanti-

tative mapping of blood volume and endothelial permeability in brain tumors," J. Magn. Reson Imaging **12**, 347–357 (2000).
[16]R. J. Gillies, Z. M. Bhujwalla, J. Evelhoch, M. Garwood, M. Neeman, S. P. Robinson, C. H. Sotak, and B. van der Saden, "Applications of magnetic resonance in model systems: Tumor biology and physiology," Neoplasia **2**(1-2) 139–151 (2000).
[17]J. F. Dunn, J. O'Hara, Y. Zaim-Wadghiri, L. H. ZhuH, M. E. Meyerand, O. Y. Grinberg, H. Hou, P. Hoopes, E. Demidenko, and H. M. Swartz, "Oxygenation of intracranial tumors with carbogen, an MR "BOLD" imaging and EPR oximetry study," J. Magn. Reson Imaging **16**(5), 511–521 (2002).
[18]R. W. Cox, "AFNI: software for analysis and visualization of functional magnetic resonance neuroimages," Comput. Biomed. Res. **29**, 162–173 (1996).
[19]Q. Shen, H. Ren, M. Fisher, J. Bouley, and T. Duong, "Dynamic tracking of acute ischemic tissue fates using improved unsupervised ISODATA analysis of high-resolution quantitative perfusion and diffusion data," J. Cereb. Blood Flow Metab. **24**, 887–897 (2004).
[20]A. J. Viera and J. M. Garrett, "Understanding Interobserver Agreement: The Kappa Statistic," Fam. Med. **37**(5), 360–363 (2005).
[21]K. E. Wallner *et al.*, "Patterns of failure follwing treatment for glioblastoma multiforme and anaplastic astrocytoma," IJROBP 40, 1141–1149 (1989).
[22]M. Law, S. Yang, J. S. Babb, E. A. Knopp, J. G. Golfinos, D. Zagzag, and G. Johnson, "Comparison of cerebral blood volume and vascular permeability from dyanamic susceptibility contrast-enhanced perfusion MR imaging with glioma grade," AJNR 25, 746–755 (2004).
[23]S. P. Robinson, P. F. J. W. Rijken, F. A. Howe, P. M. J. McSheehy, B. P. J. van der Sanden, A. Heerschap, M. Stubbs, A. J. van der Kogel, and J. R. Griffiths, "Tumor vascular architecture and function evaluated by noninvasive susceptibility MRI methods and immunohistochemistry," J. Magn. Reson Imaging **17**, 445–454 (2003).
[24]N. J. Taylor, H. Baddeley, K. A. Goodchild, M. E. B. Powell, M. Thoumine, P. J. Hoskin, H. Phillips, A. R. Padhani, and J. R. Griffiths, "BOLD MRI of human tumor oxygenation during carbogen breathing," J. Magn. Reson Imaging **14**, 156–163 (2001).
[25]D. Pauleit *et al.*, "Can the apparent diffusion coefficient be used as a non-invasive parameter to distinguish tumor tissue from peritumoral tissue in cerebral gliomas?," J. Magn. Reson Imaging **20**, 758–764 (2004).